PHYSICAL REVIEW D **90,** 065034 (2014)

Minimal model of Majoronic dark radiation and dark matter

We-Fu Chang*
Department of Physics, National Tsing Hua University, HsinChu 300, Taiwan

John N. Ng
Theory Group, TRIUMF, 4004 Wesbrook Mall, Vancouver British Columbia V6T 2A3, Canada
(Received 25 June 2014; published 30 September 2014)

We extend the singlet Majoron model of dark radiation by adding another singlet scalar of unit lepton charge. The spontaneous breaking of global $U(1)_L$ connects dark radiation with neutrino mass generation via the type-I seesaw mechanism. The model naturally has a stable scalar dark matter field. It also predicts the existence of a light scalar of mass less than 1 GeV that mixes with the Standard Model Higgs boson. We perform a numerical analysis of the parameters of the model by imposing constraints from giving correct relic abundance and satisfying bounds from direct dark matter detection, rare decays of the B meson, and invisible width of the Higgs boson. The viability of the model in accommodating the gamma rays from the Galactic center is discussed as well. The model gives rise to new rare Higgs boson decays such as four-muon final states with displaced vertices. Another unique signal is two muons and missing energy recoil against the muon pair. Our result also shows that such a bridge between dark radiation and the seesaw mechanism will put the seesaw scale in the range of 1–100 TeV.

DOI: 10.1103/PhysRevD.90.065034 PACS numbers: 14.60.St, 95.35.+d

I. INTRODUCTION

The temperature fluctuation in the cosmic microwave background radiation (CMBR) is a sensitive measure of the number of relativistic degrees of freedom present before the era of recombination. This is usually given in terms of the effective number of neutrinos, $N_{\rm eff}$, which in the Standard Model (SM) is three. Taking into account incomplete neutrino decoupling during e^+e^- annihilation and finite temperature effects leads to the SM prediction of $N_{\rm eff} = 3.046$ (see e.g. [1]). Observations thus far are consistent with this value. However, recent measurements of CMBR from the Planck satellite [2] combined with that of the Hubble constant from the Hubble Space Telescope [3] resulted in a higher value of $N_{\rm eff} = 3.83 \pm 0.54$ at 95% C.L. If one further includes data from WMAP9 [4], Atacama Cosmology Telescope [5] and the South Pole Telescope [6] into the analysis, the extracted value becomes $N_{\rm eff} = 3.62^{+0.50}_{-0.48}$ at 95% C.L. The nonzero $\triangle N_{\rm eff} \equiv N_{\rm eff} - 3.046$ can be taken as a hint of a dark radiation (DR) component beyond the expected three neutrino species at a confidence level of 2.4σ. The origin and nature of this mysterious DR is not known. One possibility is a massless or nearly massless Goldstone boson arising from the spontaneous breaking of a $U(1)$ global symmetry. A Goldstone boson will count as $4/7$ of a neutrino, and it appears to agree with observation. However, in order for the temperature of the Goldstone bosons to match with that of the neutrinos, they must remain in thermal equilibrium with ordinary matter until muon annihilation [7]. If Goldstone bosons decouple much earlier, they will contribute less than $4/7$ to $N_{\rm eff}$ as they will not be reheated but the neutrinos always will. Decoupling in the muon annihilation era yields a contribution $\triangle N_{\rm eff} = 0.39$. It is definitely interesting to investigate the nature of this global $U(1)$. Weinberg suggested that it is a new symmetry associated with the dark sector only. We believe it is worthwhile to investigate whether this global $U(1)$ can be one of the well-known accidental symmetries of the SM, i.e. the baryon or the lepton number. In [8] we make use of $U(1)_L$, the global lepton number L, and its spontaneous breaking gives rise to the Goldstone boson which is the Majoron originally studied in [9]. This allows us to make the connection between cosmic DR and neutrino mass generation such as the seesaw mechanism [10]. In so doing we can ask whether there are new constraints on the seesaw mechanism. Some other physics consequences are also studied in [8]. However, in this Majoronic DR model there is no dark matter (DM) candidate. In this paper we show that adding DM can be achieved while maintaining much of the simplicity of the model.

In the Majoronic DR model a singlet Higgs field S with lepton charge $L = 2$ is utilized to give mass to the right-handed singlet neutrino N_R by spontaneously breaking $U(1)_L$. The imaginary or axial part of this scalar field is the Goldstone boson which we identify as DR. In this paper we extend the model by adding a $L = 1$ complex scalar field Φ, a genuine scalar field which does not develop a vacuum expectation value (vev). After symmetry breaking a discrete Z_2 symmetry remains and we call that dark parity (DP). This parity will allow us to identify the lightest of the two components of Φ as the DM candidate. In this case its

*Corresponding author.
wfchang@phys.nthu.edu.tw

stability is guaranteed by DP. The details of the model are given in the next section.

While Goldstone bosons are attractive candidates for DR, there are other possibilities studied in the literature. Light sterile neutrinos were considered in [11]. In addition, right-handed neutrinos with milliweak interactions as DR were attended to in [12]. Contribution to $N_{\rm eff}$ from axion-like particles was mentioned in [13]. Connection of DR to asymmetric dark matter scenarios was studied in [14]. A more unconventional view that $\Delta N_{\rm eff}$ arises from not fully thermalized sub-eV light decay products of an exotic particle was studied in [15].

This paper is organized as follows. In Sec. II we present the detailed construction of the model. Section III is devoted to a calculation of the relic abundance of the DM particle and direct detection is discussed in Sec. IV. This is followed by examination of the constraints on the parameter space of the model from direct detection, indirect detection and other experimental constraints. The issue of galactic diffuse gamma rays is taken up in Sec. VI. Since our model makes use of SM singlet scalars, it is not surprising that it will lead to new rare Higgs decays, and this is studied in Sec. VII. Finally we give our conclusions in Sec. VIII.

II. THE MODEL

We add to the particle contents of the SM a singlet Higgs field S which carries lepton number $L = 2$ and a non-Higgssed scalar field Φ with $L = 1$. In order to implement the type-I seesaw mechanism we add the requisite minimum of two singlet Majorana right-handed neutrinos N_i, $i = 1, 2$. The new degrees of freedom together with the SM Higgs field H, lepton doublets L_i, $i = 1, 2, 3$, and their quantum numbers are listed in Table I where L denotes the charge under a global $U(1)_{\rm L}$ lepton symmetry.

With the quantum numbers assigned, Φ will not have trilinear coupling with H and it will not contribute to the Majorana masses of N_{Ri}. It will not have a Dirac mass type of couplings to the active neutrinos since it is a $SU(2)$ singlet. Thus, much of the Majoron model is not changed.

The scalar Lagrangian is

$$\begin{aligned}\mathcal{L}_{\rm scalar} &= (D_\mu H)^\dagger (D^\mu H) + (\partial_\mu S)^\dagger (\partial^\mu S) \\ &\quad + (\partial_\mu \Phi)^\dagger (\partial^\mu \Phi) - V(H, S, \Phi), \\ V(H, S, \Phi) &= -\mu^2 H^\dagger H + \lambda (H^\dagger H)^2 - \mu_s^2 S^\dagger S + \lambda_s (S^\dagger S)^2 \\ &\quad + \lambda_{SH} (S^\dagger S)(H^\dagger H) + m_\Phi^2 \Phi^\dagger \Phi + \lambda_\Phi (\Phi^\dagger \Phi)^2 \\ &\quad + \lambda_{\Phi H} (\Phi^\dagger \Phi)(H^\dagger H) + \lambda_{\Phi S} (S^\dagger S)(\Phi^\dagger \Phi) \\ &\quad + \frac{\kappa}{\sqrt{2}} [(\Phi^\dagger)^2 S + S^\dagger \Phi^2], \end{aligned} \tag{1}$$

and we take κ to be real and $m_\Phi^2 > 0$. Due to the κ term it is more convenient to work with the usual linear representation of the scalar fields. We expand the fields as follows,

$$\begin{aligned}\Phi &= \frac{1}{\sqrt{2}} (\rho + i\chi), \\ S &= \frac{1}{\sqrt{2}} (v_s + s + i\omega), \end{aligned} \tag{2}$$

and use the U gauge for the Higgs field

$$H = \begin{pmatrix} 0 \\ \frac{v+h}{\sqrt{2}} \end{pmatrix}. \tag{3}$$

The physical fields are $\hat{S} = (h, s, \rho, \chi)$ and ω is the Goldstone boson which is the Majoron. In the above basis the spin-0 mass matrix squared is

$$M^2 = \begin{pmatrix} 2\lambda v^2 & \lambda_{SH} v v_s & 0 & 0 \\ \lambda_{SH} v v_s & 2\lambda_s v_s^2 & 0 & 0 \\ 0 & 0 & m_\Phi^2 + \kappa v_s + \frac{1}{2}\lambda_{\Phi H} v^2 + \frac{1}{2}\lambda_{\Phi S} v_s^2 & 0 \\ 0 & 0 & 0 & m_\Phi^2 - \kappa v_s + \frac{1}{2}\lambda_{\Phi H} v^2 + \frac{1}{2}\lambda_{\Phi S} v_s^2 \end{pmatrix}, \tag{4}$$

and ω is massless. Note that the κ term splits the masses of ρ and χ and we require $m_\Phi^2 > |\kappa v_s| - \frac{1}{2}(\lambda_{\Phi h} v^2 + \lambda_{\Phi S} v_s^2)$.

The scalar potential becomes

$$\begin{aligned} V &= \frac{1}{2} \tilde{\hat{S}} M^2 \hat{S} + \lambda v h^3 + \frac{1}{4}\lambda h^4 + \lambda_s v_s s^3 + \lambda_s v_s \omega^2 s + \frac{1}{4}\lambda_s (s^4 + \omega^4) \\ &\quad + \frac{1}{2}\lambda_s \omega^2 s^2 + \frac{1}{2}\lambda_{SH} v_s s h^2 + \frac{1}{2}\lambda_{SH} v (s^2 + \omega^2) h + \frac{1}{4}\lambda_{SH} (s^2 + \omega^2) h^2 \\ &\quad + \frac{1}{4}\lambda_\Phi (\rho^4 + \chi^4 + 2\rho^2\chi^2) + \frac{1}{2}\lambda_{\Phi H} v (\rho^2 + \chi^2) h + \frac{1}{4}\lambda_{\Phi H} (\rho^2 + \chi^2) h^2 \\ &\quad + \frac{1}{2}\bar{\kappa} s \rho^2 + + \frac{1}{4}\lambda_{\Phi S} (s^2\rho^2 + s^2\chi^2 + \omega^2\rho^2 + \omega^2\chi^2) \\ &\quad + \frac{1}{2}(\bar{\kappa} - 2\kappa) s \chi^2 + \kappa \rho \chi \omega, \end{aligned} \tag{5}$$

TABLE I. Relevant fields and their quantum numbers.

	L	$SU(2)$	$U(1)_Y$
S	2	1	0
Φ	1	1	0
H	0	2	$\frac{1}{2}$
N_{iR}	1	1	0
L_i	1	2	$-\frac{1}{2}$

where $\bar{\kappa} = \lambda_{\Phi S} v_s + \kappa$. After spontaneous symmetry breaking of $U(1)_L$, there remains a Z_2 symmetry which we refer to as DP. It is seen by the following transformation:

$$s, \omega, h \longrightarrow s, \omega, h \qquad \rho \longrightarrow -\rho \qquad \chi \longrightarrow -\chi. \tag{6}$$

Our DP can be written as $(-1)^L$ which is coincidentally the same as the R-parity in supersymmetric models of DM. Depending on the sign of κ, either ρ or χ will be the dark matter candidate. For definiteness we choose κ to be negative; thus ρ is our DM candidate. The field ω remains massless and is the Goldstone boson which will be the DR. The two remaining scalar bosons are s, h. We can see from Eq. (4) that they form a submatrix that can be diagonalized independently of (ρ, χ). They are analyzed in Ref. [16], where the relevant Higgs bosons constraints were also presented. The mass squared eigenvalues are

$$m^2_{1,2} = \lambda v^2 + \lambda_S v_S^2 \mp \sqrt{(\lambda_S v_S^2 - \lambda v^2)^2 + \lambda_{HS}^2 v^2 v_S^2}. \tag{7}$$

The physical mass eigenstates are then

$$\begin{pmatrix} h_1 \\ h_2 \end{pmatrix} = \begin{pmatrix} \cos\theta & -\sin\theta \\ \sin\theta & \cos\theta \end{pmatrix} \begin{pmatrix} h \\ s \end{pmatrix}, \tag{8}$$

with mixing angle

$$\tan 2\theta = \frac{\lambda_{HS} v v_S}{\lambda_S v_S^2 - \lambda v^2}. \tag{9}$$

We shall identify $h_1 \equiv h_{SM}$ as the SM Higgs, which was recently discovered at the LHC to have a mass of 125 GeV. Note that for small mixing (which shall be the case below), $m^2_{h_{SM}} \approx 2\lambda v^2$ and $m_2^2 \approx 2\lambda_S v_S^2$. For all intent and purposes $h_1 \approx h$ and $h_2 \approx s$.

We can now employ the type-I seesaw mechanism to give masses to the active neutrinos. To set the notation we discuss the one family case which can be easily generalized to the three families. The $U(1)_L$ invariant interaction Lagrangian for the neutrinos is

$$-\mathcal{L}_\ell = y \bar{L}_L \tilde{H} N_R + Y \overline{N_R^c} N_R S + \text{H.c.}, \tag{10}$$

where $L = (n_L, e_L)^T$ is the SM lepton doublet and $\tilde{H} = i\sigma_2 H^*$. After symmetry breaking we get

$$-\mathcal{L}_\ell = \frac{yv}{\sqrt{2}} \overline{n_L} N_R + \frac{Y v_s}{\sqrt{2}} \overline{N_R^c} N_R + \frac{y}{\sqrt{2}} \overline{n_L} N_R h + \frac{Y}{\sqrt{2}} (s + i\omega) \overline{N_R^c} N_R + \text{H.c.} \tag{11}$$

This yields the standard seesaw neutrino mass matrix

$$\begin{pmatrix} 0 & m \\ m & M \end{pmatrix}, \tag{12}$$

where $m = \frac{yv}{2\sqrt{2}}$ and $M = \frac{Y v_s}{\sqrt{2}}$. For $\epsilon \equiv m_D/M \ll 1$, the standard type-I seesaw is operative. To leading order in ϵ, the mass eigenstates are given by

$$\nu_L = n_L + \epsilon N_R^c, \qquad \eta_R = N_R - \epsilon n_L^c, \tag{13}$$

with eigenvalues $m_\nu = \epsilon m_D$ and M, respectively, (after appropriate phase rotations). In order to obtain light active neutrino masses, $m_\nu \lesssim 0.1$ eV, we require

$$y_1 = 2^{5/4} \left(\frac{m_\nu y_2 v_s}{v} \right)^{1/2} \lesssim 3.05 \times 10^{-6} \left(\frac{y_2 v_s}{\text{TeV}} \right)^{1/2}. \tag{14}$$

As a benchmark, we take $v_s = 1$ TeV and $y_2 = 1$. Then acceptable light neutrino masses can be obtained with y_1 the size of the electron Yukawa couplings, $y_e = \frac{\sqrt{2} m_e}{v} = 2.91 \times 10^{-6}$.

Next we discuss how the neutrinos transform under DP. All SM leptons and N_R carry one lepton charge thus they are DP-odd. For the seesaw mechanism to operate, N_R needs to be heavy and will not be stable and thus cannot be a DM candidate. Although the SM charged leptons will also be DP odd this does not lead to any new phenomenon since the electroweak theory is DP conserving, and the electron remains stable. Moreover, ρ and χ do not have direct coupling to the SM leptons.

It is easy to check that the charged leptons do not couple to ω directly in the linear realization. In the nonlinear realization, the ω couples to leptons derivatively and this interaction vanishes when one of the external leptons is an on-shell Dirac fermion. In the linear representation the process $f + \bar{f} \to \omega\omega$ where f is a charged lepton will proceed via the diagrams depicted in Fig. 1.

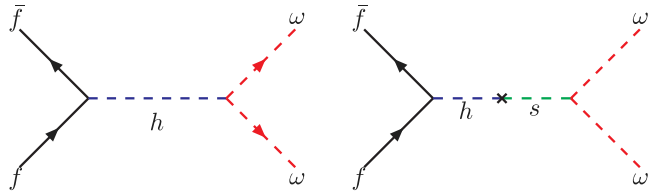

FIG. 1 (color online). Fermion-antifermion annihilation into a pair of Majorons.

Since we want the ω to act as the DR and gives $\Delta N_{\rm eff} = .39$ it should decouple from the thermal bath around the muon annihilation temperature [7]. Earlier decoupling will not yield the above $\Delta N_{\rm eff}$. In that era, it is most convenient to calculate this using the mass insertion techniques. We can take $s \simeq 4m_f^2$ and get

$$\mathcal{L}_{f\omega} \sim \frac{4\lambda_{HS} m_f^3}{M_h^2 M_s^2} \bar{f} f \omega\omega, \tag{15}$$

where $M_h^2 \simeq 2\lambda v^2$, $M_s^2 \simeq 2\lambda_s v_s^2$, and it agrees with the one obtained by using nonlinear realization [7,8] at low energies. Equation (15) allows the ω to play the role of DR. For that it has to stay in thermal equilibrium until roughly the time of muon annihilations. This requires the collision rate of ω into muons to be approximately the Hubble expansion rate at the decoupling temperature $T_{\rm dec}$,

$$\frac{\lambda_{HS}^2 m_\mu^2 T_{\rm dec}^5 m_{Pl}}{m_{h_{SM}}^4 m_{h_2}^4} \approx 1 \Longrightarrow m_{h_2} \approx 9.3\ \text{GeV} \times (T_{\rm dec}/m_\mu)^{5/4} \sqrt{|\lambda_{HS}|}, \tag{16}$$

where we take $m_{h_{SM}} = 125$ GeV. Hence we expect to have a h_2 much lighter then the Higgs which mixes with it. For notational simplicity h_1 will be called h, and h_2 will be called s.

Due to the $h - s$ mixing the Higgs boson acquires three possible new two-body decays: (a) $h \to \omega\omega$, (b) $h \to \rho\rho$ and (c) $h \to ss$. Channel (b) will open if $M_\rho < M_H/2$. (a) and (b) will add to the Higgs invisible width. As we shall see later we expect $M_s \ll M_H$ and whether (c) will lead to invisible decays depends on various parameters. Aside from those considerations the widths for the above channels are

$$\begin{aligned}
\Gamma(h \to \omega\omega) &= \frac{1}{32\pi} \frac{s_\theta^2 M_h^3}{v_s^2}, \\
\Gamma(h \to \rho\rho) &= \frac{1}{32\pi} \frac{M_\rho}{M_h^2} \sqrt{x_h - 4} [\lambda_{\Phi H} v c_\theta - s_\theta \bar{\kappa}]^2, \\
\Gamma(h \to ss) &= \frac{1}{128\pi} \frac{M_\rho}{M_h^2} \sqrt{x_h - x_s} s_{2\theta}^2 \left(\frac{s_\theta}{v} - \frac{c_\theta}{v_s}\right)^2 \times (M_h^2 + 2M_s^2)^2,
\end{aligned} \tag{17}$$

where $x_i = \frac{m_i^2}{M_\rho^2}$ and i is the particle species. We also use the notation $s_\theta = \sin\theta$ and $c_\theta = \cos\theta$.

To get a qualitative feeling for the parameters we first take the case that only (a) adds to the invisible Higgs width. From that the Higgs invisible decay branching ratio is $\lesssim 0.19$ [17] with the Higgs width at about 4.1 MeV [18], we get the Higgs invisible width to be $\lesssim 0.8$ MeV. For small mixing, this yields the constraint

$$\lambda_{SH} < 0.0128. \tag{18}$$

From Eq. (16) we thus obtain $m_s \lesssim 1.05$ GeV.

If the ρ channel is open we get instead

$$\frac{1}{2} \lambda_{\Phi H}^2 \sqrt{1 - 4/x_H} + \lambda_{SH}^2 < 1.27 \times 10^{-4}. \tag{19}$$

This implies $\lambda_{\Phi H} \simeq \lambda_{SH}$. It is easy to see that scalar s has mass of O(GeV) or less still holds qualitatively.

The signal from the decay $h \to ss$ will depend on M_s, which dictates the decay modes of s. The relevant modes are s into light quarks and leptons, ω's and gluons. The invisible width is

$$\Gamma(s \to \omega\omega) = \frac{1}{32\pi} \frac{c_\theta^2 M_s^3}{v_s^2}, \tag{20}$$

whereas the two fermions' width is

$$\Gamma(s \to f\bar{f}) = \frac{M_s}{8\pi} N_c^f \beta_f^3 \left(\frac{m_f s_\theta}{v}\right)^2, \tag{21}$$

where $\beta_f = \sqrt{1 - \frac{4m_f^2}{M_s^2}}$ and N_c^f denotes the color of the fermion.

How large a contribution of this to the Higgs invisible decay depends on the relative size of $\frac{M_s}{v_s}$ and θ. Nevertheless it is clear this will not change the result $M_s \lesssim$ O (GeV). For $M_s \lesssim 1$ GeV we also have

$$\Gamma_{\mu^+\mu^-} : \Gamma_{u\bar{u},d\bar{d}} : \Gamma_{gg} = m_\mu^2 \beta_\mu^3 : 3m_{u,d}^2 \beta_\pi^2 : \left(\frac{\alpha_s}{\pi}\right)^2 M_s^2 \left(\frac{6 - 2\beta_\pi^3}{3}\right)^2, \tag{22}$$

where we have neglected the kaon modes which are kinematically suppressed. To close this section we mention that some low-energy consequences of this light scalar have been explored in [8].

III. DARK MATTER AND ITS RELIC ABUNDANCE

A. DM annihilation channels

In our model, due to the Z_2 DP the lighter of ρ and χ will be the DM. Without loss of generality we choose it to be ρ. Then χ can decay into ρ and ω. Hence there is only one DM candidate. Note that $M_\rho^2 - M_\chi^2 = 2\kappa v_s$ and the mass difference is not necessarily small. The relic density of ρ can be calculated by evaluating the rate of a pair of ρ annihilating into SM particles as well as new scalars that are lighter than ρ. The SM channels are depicted in Fig. 2 and are open if it is heavy enough. Two DMs can annihilate into lighter scalars as well as the Majorons. These reactions are given below. Since the mixing between the Higgs and the light scalar is small, we can neglect it here and only the diagonal terms are important. We note that there can also be the coannihilation of ρ and χ into scalars and Majoron but these will require κ to be fine-tuned to very small values. The effect of the neutrino sector on DM relic abundance depends on the mass M_R of N_R. We are interested in the

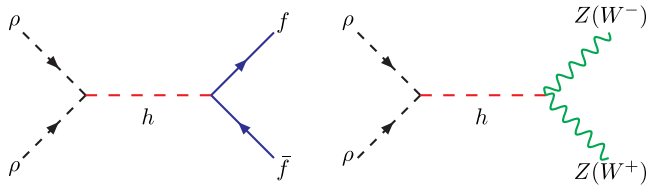

FIG. 2 (color online). $\rho\rho$ annihilation into SM particles.

case of $M_\rho < M_R$ then the neutrino sector has minimal effect on DM relic abundance.

B. Relic density

The evolution of the comoving particle density is given by the Boltzmann equation

$$\frac{1}{n_{\rm eq}}\frac{\partial n}{\partial t} = \Gamma\cdot\left(\frac{n^2}{n_{\rm eq}^2}-1\right) - 3H\frac{n}{n_{\rm eq}}, \tag{23}$$

where n is the particle density at time t and $n_{\rm eq}$ is the density at equilibrium, H is the Hubble expansion rate and Γ parametrizes the interaction rate, $\Gamma = \langle\sigma v\rangle n_{\rm eq}$, with $\langle\sigma v\rangle$ the thermally averaged annihilation cross section. By solving numerically the above equation, one can find the temperature at which particles depart from equilibrium and freeze out. Crudely speaking since time is inversely proportional to temperature the above equation can be viewed as an evolution equation with respect to temperature. The freeze-out temperature T_f is given by

$$x_f \equiv \frac{M_\rho}{T_f} = \ln\left(0.038 g_X\langle\sigma v\rangle M_\rho M_{\rm Pl}\sqrt{\frac{x_f}{g_*}}\right), \tag{24}$$

where $M_{\rm Pl}$ is the Planck mass and g_* is the effective number of relativistic degrees of freedom at temperature T. For large $x_f \sim 20$ one can neglect the x_f factor in the logarithm. Once we know $\langle\sigma v\rangle$, we can calculate the freeze-out temperature of X with a given mass.

It is now straightforward to calculate the $\rho\rho$ annihilation cross sections to various final states. The Feynman diagrams are given in Figs. 2, 3. For completeness, the results we get for a general mixing are

$$\begin{aligned}
(\sigma v)_{ss} &= \frac{1}{64\pi}\frac{\sqrt{1-x_s}}{M_\rho^2}\left[q_{SS} + \frac{g_{\rho H}\lambda_{HSS}}{M_\rho^2(4-x_H)} + \frac{g_{\rho S}\lambda_{SSS}}{M_\rho^2(4-x_S)} - \frac{2g_{\rho S}^2}{M_\rho^2(2-x_s)}\right]^2,\\
(\sigma v)_{HH} &= \frac{1}{64\pi}\frac{\sqrt{1-x_H}}{M_\rho^2}\left[q_{HH} + \frac{g_{\rho H}\lambda_{HHH}}{M_\rho^2(4-x_H)} + \frac{g_{\rho S}\lambda_{SHH}}{M_\rho^2(4-x_S)} - \frac{2g_{\rho H}^2}{M_\rho^2(2-x_H)}\right]^2,\\
(\sigma v)_{Hs} &= \frac{1}{32\pi}\frac{\Delta}{M_\rho^2}\left[q_{HS} + \frac{g_{\rho H}\lambda_{SHH}}{M_\rho^2(4-x_H)} + \frac{g_{\rho S}\lambda_{HSS}}{M_\rho^2(4-x_S)} - \frac{4g_{\rho H}g_{\rho S}}{M_\rho^2(4-x_H-x_s)}\right]^2,\\
(\sigma v)_{\omega\omega} &= \frac{1}{64\pi M_\rho^2}\left[\frac{g_{\rho H}g_{\omega H}}{M_\rho^2(4-x_H)} + \frac{g_{\rho S}g_{\omega S}}{M_\rho^2(4-x_S)} + \lambda_{\Phi S} - \frac{2\kappa^2}{M_\rho^2(1+x_\chi)}\right]^2,\\
(\sigma v)_{WW} &= \frac{1}{8\pi}\frac{\lambda_{\Phi H}^2}{M_\rho^2}\sqrt{1-x_W}[4-4x_W+3x_W^2]\left[\frac{c_\theta^2}{(4-x_H)} + \frac{s_\theta^2}{(4-x_S)}\right]^2,\\
(\sigma v)_{ZZ} &= \frac{1}{16\pi}\frac{\lambda_{\Phi H}^2}{M_\rho^2}\sqrt{1-x_Z}[4-4x_Z+3x_Z^2]\left[\frac{c_\theta^2}{(4-x_H)} + \frac{s_\theta^2}{(4-x_S)}\right]^2,\\
(\sigma v)_{f\bar f} &= \frac{N_c}{4\pi}\frac{\lambda_{\Phi H}^2 x_f}{M_\rho^2}(1-x_f)^{\frac{3}{2}}\left[\frac{c_\theta^2}{(4-x_H)} + \frac{s_\theta^2}{(4-x_S)}\right]^2,
\end{aligned} \tag{25}$$

where $\Delta^2 = 1 + \frac{1}{16}x_H^2 + \frac{1}{16}x_s^2 - \frac{1}{8}x_H x_s - \frac{1}{2}x_H - \frac{1}{2}x_s$, $x_i = \frac{M_i^2}{M_\rho^2}$ for $i = W, Z, H, f, S, \chi$, and the subscripts denote the final state. The coupling in the scalar mass basis are given as

$$\begin{aligned}
q_{SS} &= \lambda_{\Phi S}c_\theta^2 + \lambda_{\Phi H}s_\theta^2, \qquad q_{HH} = \lambda_{\Phi S}s_\theta^2 + \lambda_{\Phi H}c_\theta^2, \qquad q_{HS} = (\lambda_{\Phi H} - \lambda_{\Phi S})c_\theta s_\theta,\\
g_{\rho S} &= \bar\kappa c_\theta + \lambda_{\Phi H} v s_\theta, \qquad g_{\rho H} = -\bar\kappa s_\theta + \lambda_{\Phi H} v c_\theta,\\
g_{\omega S} &= \lambda_{SH} v c_\theta - 2\lambda_S v_S s_\theta, \qquad g_{\omega H} = \lambda_{SH} v s_\theta + 2\lambda_S v_S c_\theta,\\
\lambda_{HHH} &= 6\lambda v c_\theta^3 - 6\lambda_S v_S s_\theta^3 + 3\lambda_{SH} s_\theta c_\theta (v s_\theta - v_S c_\theta),\\
\lambda_{SSS} &= 6\lambda v s_\theta^3 + 6\lambda_S v_S c_\theta^3 + 3\lambda_{SH} s_\theta c_\theta (v_S s_\theta + v c_\theta),\\
\lambda_{SHH} &= 6 s_\theta c_\theta(\lambda v c_\theta + \lambda_S v_S s_\theta) + \lambda_{SH} v_S (c_\theta^3 - 2 s_\theta^2 c_\theta) + \lambda_{SH} v (s_\theta^3 - 2 s_\theta c_\theta^2),\\
\lambda_{HSS} &= 6 s_\theta c_\theta(\lambda v s_\theta - \lambda_S v_S c_\theta) + \lambda_{SH} v_S (-s_\theta^3 + 2 s_\theta c_\theta^2) + \lambda_{SH} v (c_\theta^3 - 2 s_\theta^2 c_\theta).
\end{aligned} \tag{26}$$

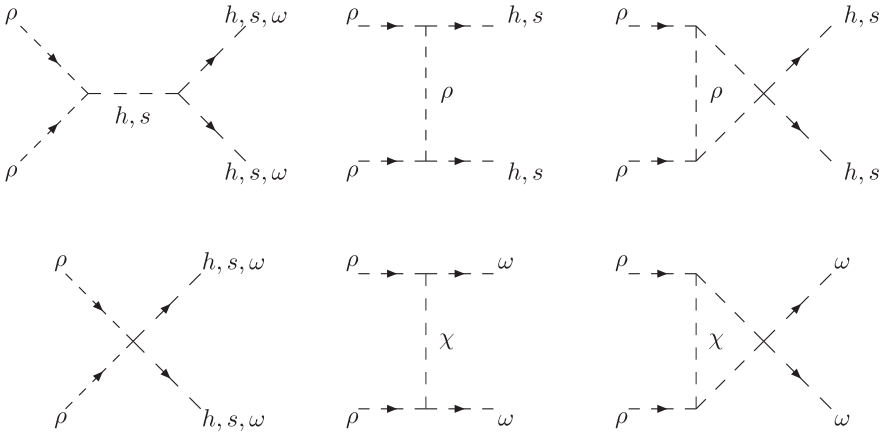

FIG. 3. $\rho\rho$ to a pair of SM Higgs, light scalars and Majorons.

For high temperatures these will give $\langle\sigma v\rangle$. It is well known that in order to get the correct relic density the total $\langle\sigma v\rangle$ should be approximately 3×10^{-26} cm^3/s. Due to the number of unknown parameters a numerical scan is required for the correct relic density. This will be given in Sec. V.

IV. DIRECT DETECTION

The DM candidate could be detected by measuring the energy deposited in a low background detector by the scattering of ρ with a nucleus of the detector. Since ρ is a scalar there are only spin independent scattering via t-channel exchange of virtual h and s. This is depicted in Fig. 4. The cross section is

$$\sigma_{\rho n}=\frac{G_F M_n^2\eta^2 m_r^2(n,\rho)}{4\sqrt{2}\pi M_\rho^2 M_H^2\lambda}\times\left[\lambda_{\Phi H}\left(c_\theta^2+s_\theta^2\left(\frac{M_h}{M_s}\right)^2\right)-s_\theta c_\theta\frac{\bar{\kappa}}{v}\left(1-\left(\frac{M_h}{M_s}\right)^2\right)\right]^2, \tag{27}$$

where the reduced mass is

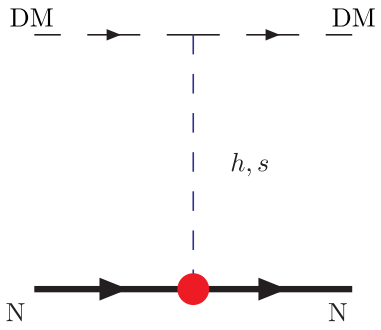

FIG. 4 (color online). Leading channel for DM-nucleon scattering via Higgs and light scalar exchange. DM is ρ.

$$m_r(n,\rho)=\frac{M_\rho M_n}{M_\rho+M_n}, \tag{28}$$

and M_n is the nucleon mass. For a qualitative estimation we take $\eta=0.3$ in our numerical analysis and ignore all the possible effects from isospin breaking or the strange-quark content which can be accounted for (see for example [19]). Since s is very light compared to the Higgs boson its contribution cannot be neglected. Hence, the direct detection sets a strong constraint on the parameters combination $\frac{\bar{\kappa}}{v}s_{2\theta}$.

V. PARAMETERS SCAN AND NUMERICAL ANALYSIS

The scalar potential introduces 8 more parameters to the SM. We perform a global numerical scan to investigate the general properties of this model in different regions of parameter space. We employ 4000 randomly generated points. The parameters scan is performed for $m_\rho\in[6,2000]$ GeV as follow:

(1) The mass of light scalar M_s is randomly chosen between 0.0 and 1.0 GeV. Such a light scalar is required if the Goldstone is associated with a dark $U(1)$ global symmetry.

(2) So as not to miss any possible solution, the mixing, $\sin\theta$, is randomly picked between ±0.01. This value is dictated by constraints on light scalars mixing with the Higgs from rare B-meson decays [20]. With the above inputs, we fix $|\lambda_{SH}|=(M_s/22.11\text{ GeV})^2$ by the requirement that the Majoron decouples from the primordial plasma at around twice the muon mass ($T_{\rm dec}\sim 2m_\mu$). This does not change $\Delta N_{\rm eff}=.39$ as compared to using $T_{\rm dec}\sim m_\mu$ [7] and allows us to probe a larger parameter space. Also its sign is opposite to that of $\sin\theta$. This is to be viewed as a benchmark point and its exact value is unknown since it depends on the actual decoupling temperature.

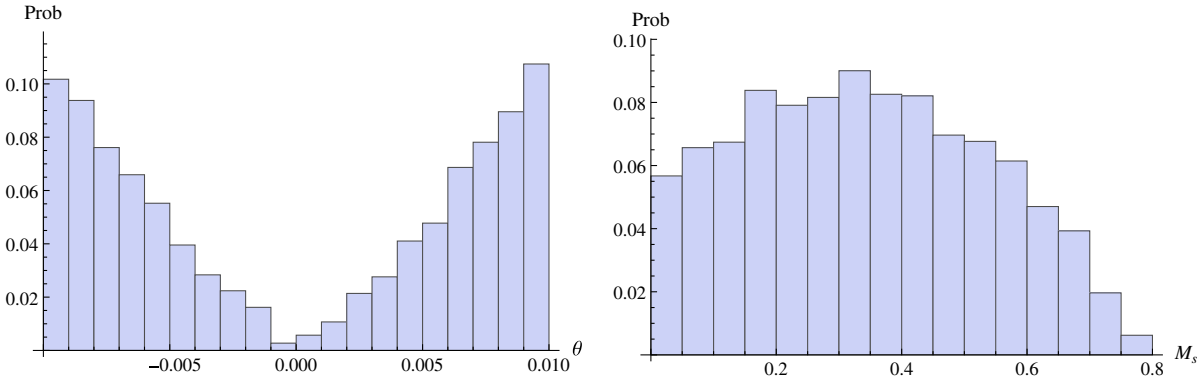

FIG. 5 (color online). The probability distribution of θ (Left Panel) and M_S (Right Panel) of all viable parameter configurations.

From the mass diagonalization, two parameters in the scalar potential and v_S can be expressed in terms of mass eigenvalues, $M_H = 125$ GeV, M_s, and the mixing,

$$\lambda = \frac{(M_H^2 c_\theta^2 + M_s^2 s_\theta^2)}{2v^2}, \qquad \lambda_S = \frac{(M_s^2 c_\theta^2 + M_H^2 s_\theta^2)}{2v_S^2},$$
$$v_S = \frac{s_\theta c_\theta}{\lambda_{SH} v}(M_s^2 - M_H^2). \tag{29}$$

(3) Next, we allow $\bar{\kappa}$ to be randomly chosen in the region between $-v$ and $+v$.
(4) Then, $\lambda_{\Phi S}$ is randomly chosen between $-4\sqrt{\pi\lambda_S}$ and 4π. Since we limit our discussion to the perturbative regime so the upper bound of any dimensionless coupling is set to be 4π. The lower bound is derived from that $(4\lambda_S\lambda_\Phi - \lambda_{\Phi S}^2) > 0$, which is the positivity requirement of the scalar potential, with the largest $\lambda_\phi = 4\pi$. And it is further required to satisfy the condition that $\kappa = \bar{\kappa} - \lambda_{\phi S} v_s < 0$. That κ is negative is because we pick ρ to be the dark matter. And the mass of χ is determined to be $M_\chi = \sqrt{M_\rho^2 - 2\kappa v_S}$.
(5) Finally, we allow $\lambda_{\phi H}$ to be randomly chosen between $-4\sqrt{\pi\lambda}$ and 4π for the same reason as in the case of $\lambda_{\phi S}$.
(6) λ_Φ does not enter into the calculations of the observables here. It remains unconstrained.

The program will register the points which satisfy all the following four criteria:

(i) $(M_\rho^2 + M_\chi^2 - \lambda_{\Phi H}^2 v^2 - \lambda_{\Phi S}^2 v_S^2) > 0$ so that $M_\Phi^2 > 0$.
(ii) The SM Higgs invisible decay width $\Gamma_{\rm inv}^h < 0.8$ MeV.
(iii) The thermal average annihilation cross section is within the range $(2.5 \pm 0.1) \times 10^{-9}$ (GeV)$^{-2}$.
(iv) The spin-independent elastic ρ-nucleon scattering cross section, Eq. (27), is smaller than the LUX 90% confidence limit [21].

First of all, we found that it is less probable to find solutions with very small mixing angle. Moreover, even we allow the M_S to be chosen between 0.0 and 1.0 GeV, the resulting M_S is cut off at around 0.8 GeV with a smooth distribution peaks at around 0.4 GeV. Both θ and M_S are insensitive to M_ρ (see Fig. 5).

The $\bar{\kappa}$ values for points which successfully stay under the direct search bound turn out to be small comparing to the

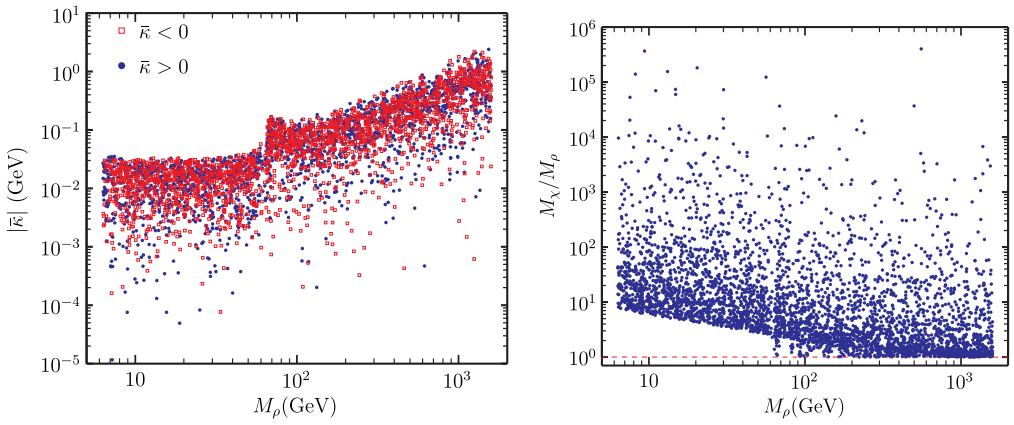

FIG. 6 (color online). Left panel: The distribution of $\bar{\kappa}$ vs M_ρ. Right panel: The mass ratio of two Z_2-odd particles vs M_ρ.

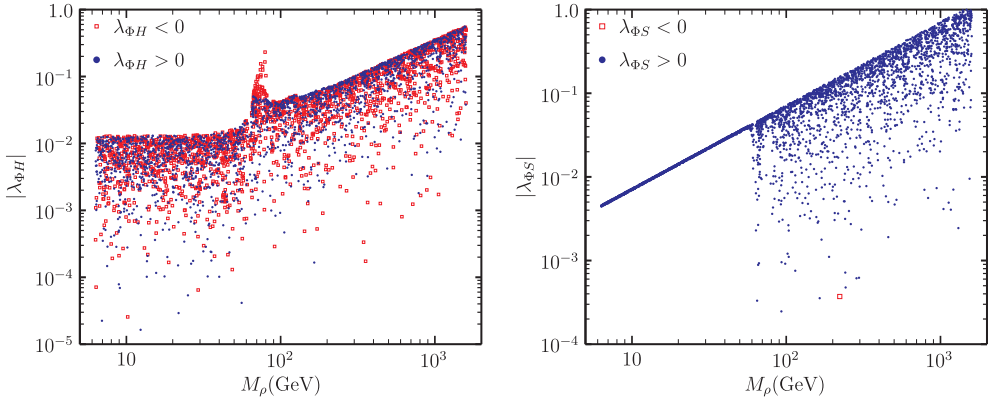

FIG. 7 (color online). $\lambda_{\phi H}$ (left panel) and $\lambda_{\phi S}$ (right panel) vs M_ρ.

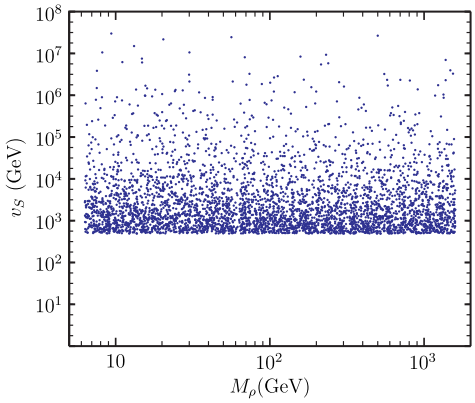

FIG. 8 (color online). The lepton number violating scale v_S vs M_ρ.

electroweak scale v, from $|\bar{\kappa}| \lesssim 0.02$ GeV for $M_\rho < M_H/2$ to $\lesssim 3$ GeV for $M_\rho \sim 2$ TeV (see the left panel of Fig. 6). Our scan shows that it seems to have equal probability to be either positive or negative. The mass of the next to lightest Z_2-odd particle has a wide range of distribution (see the right panel in Fig. 6). In general, M_χ tend to be close to M_ρ at large $M_\rho (> M_H/2)$, and the mass ratio M_χ/M_ρ gets larger as M_ρ gets smaller. The most probable band follows a rough relation $M_\chi/M_\rho \sim 3 \times (1\ \text{TeV}/M_\rho)^{1/2}$. And this result shows that for DM heavier than ~1 TeV one also needs to take the coannihilation processes into account.

The distribution of $\lambda_{\Phi H}$ and $\lambda_{\Phi S}$ for different M_ρ are compared in Fig. 7. The distribution of $\lambda_{\Phi H}$ seems to be symmetric for either sign except at around $M_\rho \sim M_H/2$ where larger value of negative $\lambda_{\Phi H}$ is preferred over the positive one. On the other hand, only about 0.03% of successful solutions have negative $\lambda_{\Phi S}$ (red squares in the figure) due to that $\lambda_S \sim (M_S/v_S)^2/2$ is very small which results in a tight lower bound for negative $\lambda_{\Phi S}$. It is easy to see that the lighter the ρ, the smaller $|\lambda_{\Phi H}|$ and $\lambda_{\Phi S}$. When $M_\rho < M_H/2$, the $\lambda_{\Phi S}$ roughly follows a scaling law that $\lambda_{\Phi S} \propto M_\rho$.

The result of our scan shows that v_s is insensitive to M_ρ (see Fig. 8). The lepton number breaking scale generally peaks at around 0.6–3 TeV and extends to around 10^5 TeV with monotonically decreasing probability. This puts the right-handed neutrino N_R within reach for LHC searches. However, a detail study will be needed as the background for heavy neutrinos searches at the LHC is expected to be large or even prohibitive.

In Fig. 9, $\langle\sigma_S v\rangle/\langle\sigma v\rangle_{\text{total}}$ and $\langle\sigma_\omega v\rangle/\langle\sigma v\rangle_{\text{total}}$ are displayed. It is easy to see that $\rho\rho \to ss$ is the dominant

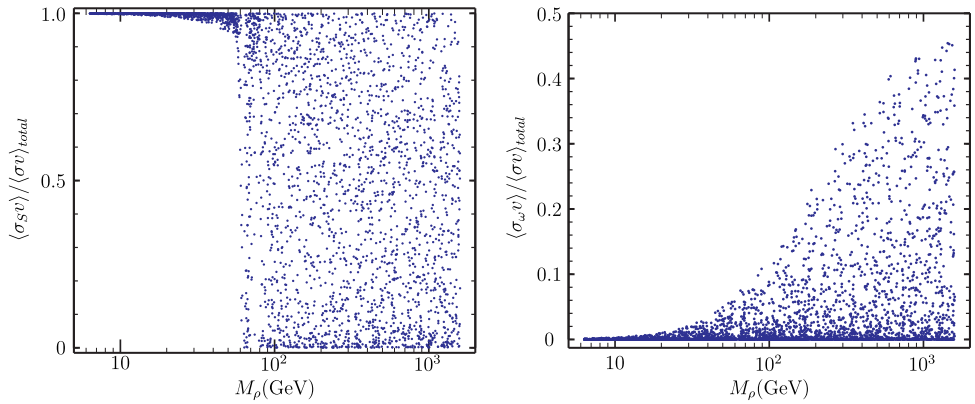

FIG. 9 (color online). $\langle\sigma_S v\rangle/\langle\sigma v\rangle_{\text{total}}$ (left panel) and $\langle\sigma_\omega v\rangle/\langle\sigma v\rangle_{\text{total}}$ (right panel) vs M_ρ.

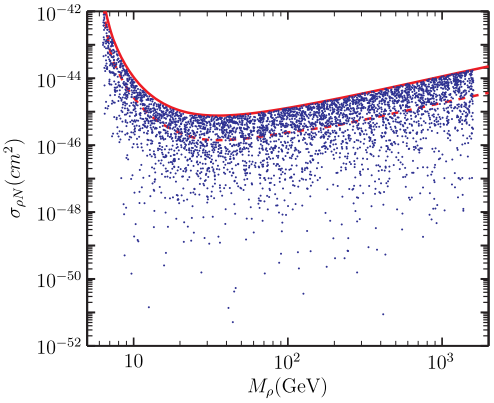

FIG. 10 (color online). Spin-independent elastic ρ-nucleon scattering cross section vs M_ρ. Where the solid line is the current LUX limit and the dashed line is the LUX 300-day projected sensitivity.

annihilation channel when $M_\rho < M_H/2$. On the other hand, the $\rho\rho \to \omega\omega$ annihilation channel starts to contribute when $M_\rho > M_H/2$ with chances to be sizable when M_ρ becomes heavier. Nevertheless, the $\rho\rho \to \omega\omega$ channel is usually insignificant in most of the parameter space. Therefore, when $M_\rho > M_H/2$, the processes of dark matter annihilate into ss and the SM particles pair are the major players determining the thermal dark matter relic density.

Finally, the resulting spin-independent elastic ρ-nucleon scattering cross section v.s. M_ρ is displayed in Fig. 10, where the LUX 90% confidence limit can be clearly seen. Most of the data points are within the range between the current LUX limit and one order smaller than the current limit which can be probed with the LUX 300-day projected sensitivity.

VI. GAMMA RAYS FROM THE GALACTIC CENTER

A recent study indicates that the low-energy (∼1–3 GeV) gamma-ray excess at the Galactic center can be accommodated by a 30–40 GeV dark matter particle annihilating into $b\bar{b}$ with an annihilation cross section of $\langle\sigma v\rangle = (1.4\text{–}2.0) \times 10^{-26}$ cm^3/s [22]. In this section we shall see whether the low-energy gamma-ray excess at the Galactic center can be accommodated with $M_\rho \sim$ 30–40 GeV in our model (see [23] for a discussion on other scenarios with the same kinematics.) As discussed in previous section, $\rho\rho \to ss$ will then be the dominant annihilation channel. Since the model predicts that the light scalar s has mass $M_s < 1$ GeV, it can only decay into light quarks or gluons at the parton level. Thus, we will discuss and compare the gamma-ray spectrum generated from the decay of s with energy ∼30–40 GeV to that of the benchmark scenario in [22].

The gamma-ray spectrum produced from dark matter annihilating into $f\bar{f}$ is given by

$$\frac{d\Phi_\gamma}{d\Omega dE_\gamma} = \sum_i \frac{dN_\gamma^i}{dE_\gamma}\frac{\langle\sigma_i v\rangle}{4\pi M_{\rm DM}^2} \times \left[B \times \int_{\text{line of sight}} \rho_{\rm DM}^2 dl\right], \tag{30}$$

where i represents the final state particle specie, $d\Omega$ is the solid angle seen from the earth, $\rho_{\rm DM}$ is the dark matter mass density, and the boost factor is defined as $B \equiv \langle\rho_{\rm DM}^2\rangle/\langle\rho_{\rm DM}\rangle^2$. The booster factor is close to its minimum = 1.0 when fluctuation of the Galactic dark matter mass density is small. If there is only one kind of dark matter, the dark matter number density will be $\rho_{\rm DM}/M_{\rm DM}$ and that explains the $M_{\rm DM}^2$ factor in the denominator. In the square bracket, the boost factor and the $\rho_{\rm DM}^2$ integral along the line of sight are purely astronomical and strongly model dependent. Here $\frac{dN_\gamma^i}{dE_\gamma}$ is the gamma-ray spectrum produced by the energetic quarks or W/Z boson with initial energy $E_i = M_{\rm DM}$ which hadronizes into π^0 and other mesons and they decay into photons subsequently. With the same initial energy, the top and bottom pairs yield the softer gamma rays, and light quark or gluon pairs yield the harder gamma rays. The gamma-ray spectrum produced by W and Z is in between the spectrum from the light quark and heavy quark. This function can only be fitted from experiments and have been encoded into many computer programs. For a ballpark estimation, we adopt a simple approximation proposed by [24]:

$$\frac{dN_\gamma^i}{dE_\gamma} \sim \frac{a_i (M_{\rm DM})^{0.5}}{(E_\gamma)^{1.5}} \times e^{-b_i E_\gamma/M_{\rm DM}}, \tag{31}$$

with $(a,b) = \{(1.0, 10.7), (1.1, 15.1), (0.95, 6.5), (0.73, 7.76)\}$ for $i = \{b\bar{b}, t\bar{t}, u\bar{u}, W^+W^-/ZZ\}$. We shall make use of this approximation and estimate the gamma rays produced from $\rho\rho \to ss$, where s subsequently decays into light quarks or gluons [so we take $(a,b) = (0.95, 6.5)$].

From the rest frame of s, we boost the isotropically distributed $s \to q\bar{q}, gg$ to energy $E_s = M_\rho$ so that the energy carried by quark or gluon in the dark matter annihilation center-of-mass (c.m.) frame is in the range between $E_f^{\rm min} = (M_\rho/2)[1 - \sqrt{1-(M_s/M_\rho)^2}\sqrt{1-(2m_f/M_s)^2}]$ and $E_f^{\rm max} = (M_\rho/2)[1 + \sqrt{1-(M_s/M_\rho)^2}\sqrt{1-(2m_f/M_s)^2}]$, where m_f is the mass of quark and 0 for gluon. After averaging over all possible direction, we obtain the following normalized differential probability of finding a light quark or gluon with energy E_f in the c.m. frame,

$$\frac{dP_s}{dE_f} = \frac{4}{\pi M_\rho}\frac{\sqrt{(1-\frac{M_s^2}{M_\rho^2})(1-\frac{4m_f^2}{M_s^2}) - (1-\frac{2E_f}{M_\rho})^2}}{(1-\frac{m_S^2}{M_\rho^2})(1-\frac{4m_f^2}{M_s^2})}, \tag{32}$$

which peaks at $E_f = M_\rho/2$ and smoothly drops to zero at $E_f^{\rm max}$ and $E_f^{\rm min}$. Notice that E_f can be viewed as the dark

matter with an effective mass $M_{\rm DM}^{\rm eff} = E_f$ annihilating into $f\bar{f}$. Hence, one can convolute this distribution with the photon spectrum function and the contribution to the gamma-ray spectrum from $\rho\rho \to ss$ can be expressed as

$$\frac{d\Phi_\gamma}{d\Omega dE_\gamma} = \left[\int_{E_f^{\rm min}}^{E_f^{\rm max}} dE_f \frac{a_s (E_f)^{0.5}}{(E_\gamma)^{1.5}} e^{-\frac{b_S E_\gamma}{E_f}} \left(2\frac{dP_s}{dE_f}\right)\right] \times \frac{Br_h \langle\sigma_S v\rangle \times B}{4\pi M_\rho^2} \int_{\rm l.o.s.} \rho_{\rm DM}^2 dl, \quad (33)$$

where Br_h is the hadronic decay branching ratio of s. The factor 2 associated the differential probability is to account for that there are 4 final light quarks or gluons from the two decaying s. We will use Eq. (22) to approximate $Br_h\langle\sigma_S v\rangle$. Since Eq. (30) can be factorized into an astrophysical part and the particle physics part, we concentrate on the particle physics component only and adopt the best fit from [22]. We use Eq. (31) for the gamma-ray spectrum from a dark matter of mass 35 GeV with an annihilating cross section into $b\bar{b}$ of 1.42×10^{-9} $(\text{GeV})^{-2}$ as the benchmark. We found that in our model $M_\rho = 37.30$ GeV and $B \times Br_h = 0.507$ give the best fit to the benchmark spectrum between energy 0.3–30 GeV where we equally divide the energy logarithm into 12 bins and the relative uncertainty is about 3% for each data point (see Fig. 7 in [22]). On the other hand, the best fit of our model has $M_\rho = 36.53$ GeV and $B \times Br_h = 0.499$ if we try to best match the benchmark spectrum between a narrower range 0.3–10.0 GeV (see Fig. 11 for the comparisons). Our best fit has a slightly harder spectrum at $E_\gamma = 10$ GeV, which is actually better than the benchmark spectrum (see Fig. 7 in [22]).

With the target range set, we zoom in our numerical search and focus on the points with $M_\rho = 37.0 \pm 5.0$ GeV. For $M_s > (M_K - m_\pi)$, the $B \to Ks \to K\mu\bar{\mu}$ and $B \to Ks \to K + (\text{nothing})$ experiments constrain θ to be

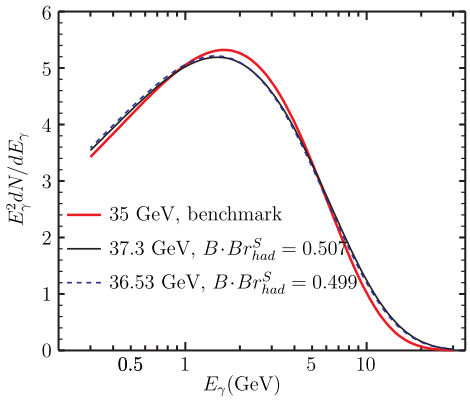

FIG. 11 (color online). Comparison of the diffuse gamma-ray spectrum $E^2 dN/dE$ with arbitrary unit from the benchmark 35 GeV DM and $\langle\sigma_b v\rangle = 1.42 \times 10^{-9}$ $(\text{GeV})^{-2}$ (red), $M_\rho = 37.30$ GeV and $B \times Br_h = 0.507$ in our model (black), and $M_\rho = 36.53$ GeV and $B \times Br_h = 0.499$ in our model (blue dash).

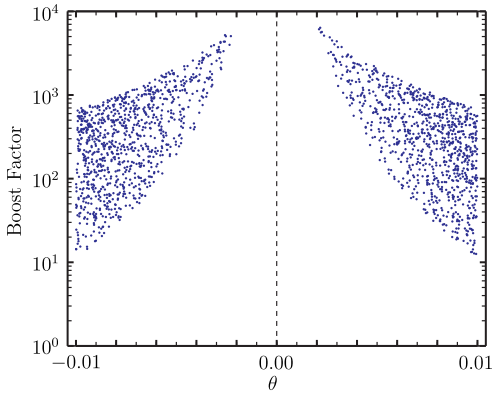

FIG. 12 (color online). The boost factor needed for $m_S > M_K - m_\pi$ to get the best-fit benchmark as a function of θ.

$\lesssim 0.01$ [20], and the corresponding boost factor ranges from ~10 to 2000, depending on the mixing (see Fig. 12).

If a smaller boost factor is preferred, it looks like the model needs to be stretched to simultaneously meet the rare B decay limits and the Galactic center gamma-ray excess. However, the boost factor is very sensitive to the decoupling temperature, $T_{\rm dec}$ [see Eq. (16)]. For example, if the decoupling temperature is slightly raised to $T_{\rm dec} \sim 2.2 m_\mu$ from $2.0 m_\mu$, the smallest B at $|\theta| \sim 0.01$ can be pushed down to ~6.0 from ~13.0 for $T_{\rm dec} \sim 2.0 m_\mu$. Given the large uncertainties in astrophysics, cosmology, and hadronic form factors, our model can accommodate the Galactic center gamma ray with a ~40 GeV ρ and satisfy the B-decay limits at the same time. However, the constraints are quite tight and a very small mixing and a higher decoupling temperature are preferred if the model is to fit the gamma rays from the Galactic center data as it stands now.

VII. RARE HIGGS BOSON DECAYS

Our model belongs to the category of Higgs portal models [25,26] in which the dark sector communicates with the SM via Higgs couplings only. The characteristic

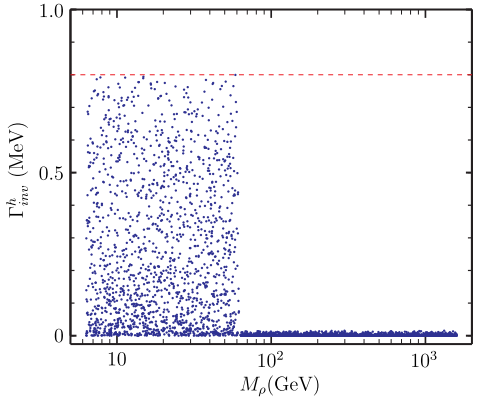

FIG. 13 (color online). SM Higgs invisible decay width $\Gamma^H_{\rm inv}$ as a function of m_ρ.

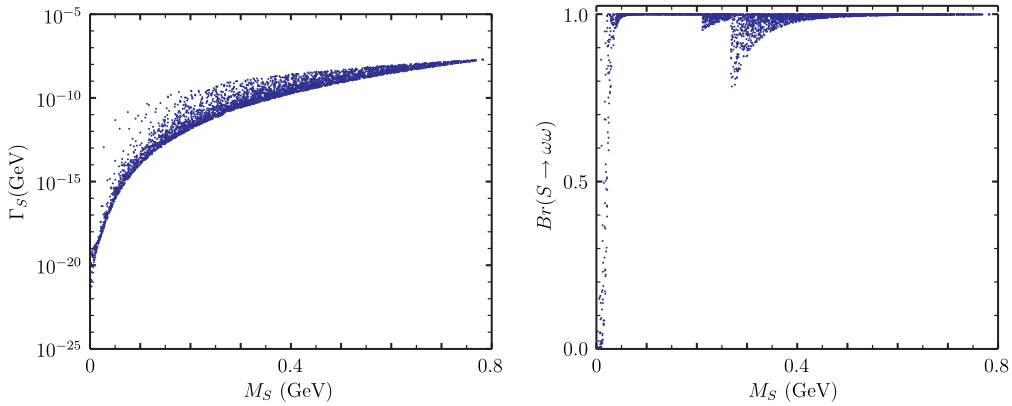

FIG. 14 (color online). Left panel: light scalar s decay width vs M_s, Right panel: invisible decay branching ratio vs M_s.

signatures are new rare Higgs decays. The new decay modes comes from (a) $h \to \omega\omega$ and (b) $h \to \rho\rho$ and (c) $h \to ss$. All three channels will give rise to $\Gamma_{\rm inv}$ for the Higgs with s decaying into a pair of ω's. In our parameter scan we require the invisible decay to concur with the experimental limit. The scatter plot given in Fig. 13 shows the preferred values. $\Gamma_{\rm inv}$ is clearly divided into two regions with the boundary at around $M_\rho = M_H/2$.

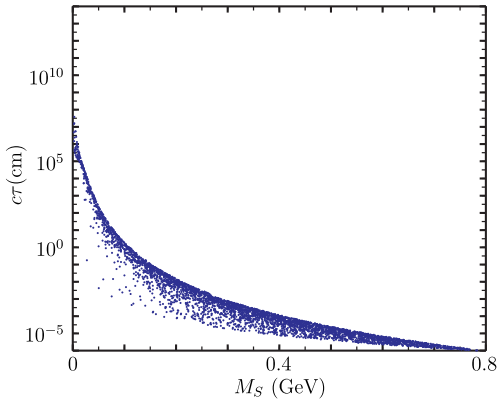

FIG. 15 (color online). Expected $c\tau$ (in cm) as a function of m_s.

For $M_\rho > M_H/2$, the model prefers a small invisible decay width, on the other hand, $\Gamma_{\rm inv}$ could be as large as the input limit, 0.8 MeV, for $M_\rho < M_H/2$. Although this not a robust prediction it can be used as a check if other signals are seen.

Other interesting Higgs boson decays comes from process-(c) and s subsequently decays into lepton pairs, hadrons or two photons depending on its mass. Since s is light and have a long lifetime displaced vertices is a clear possibility. Previously this interesting signal is considered in the context of supersymmetric models [27], leptoquark models [28], and heavy neutrino searches [29]. Here the displaced vertices originates from the Higgs boson decays. In Fig. 14, data points are displayed to show the decay width and invisible decay branching ratio for $s \to \omega\omega$ as a function of M_s. Both the decay width and invisible decay branching ratio of s are quite independent of the dark matter mass, M_ρ. This is because the s decays can be completely determined by θ, M_s, and v_s. One can see the jumps in $Br(s \to \omega\omega)$ at the $M_s = 2m_\mu$ and $M_s = 2M_\pi$ thresholds. The corresponding decay vertex displacement ranges from $\sim(M_H/2M_s) \times 10^{-5}$ cm for $M_s \sim 0.8$ GeV to $\sim(M_H/2M_s) \times 1$ cm for $M_s \sim 0.1$ GeV (see Fig. 15). The $s \to e^+e^-$ and $s \to 2\gamma$ decays are almost always overwhelmed by the $s \to \omega\omega$ channel.

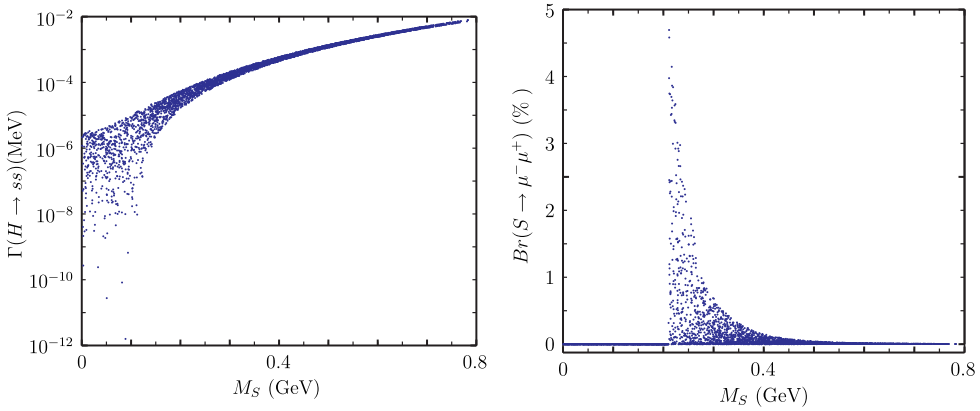

FIG. 16 (color online). Decay width $\Gamma(h \to ss)$ in MeV (left panel) and Br$(s \to \mu\mu)$ (right panel).

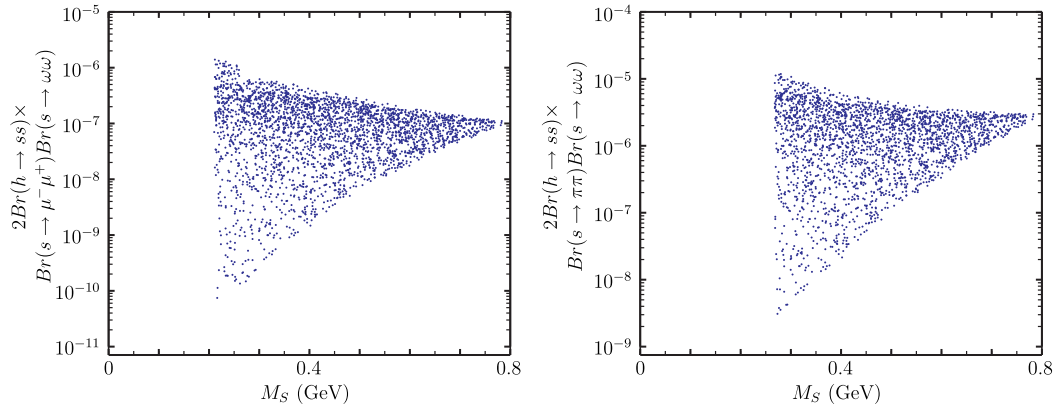

FIG. 17 (color online). The branching ratios for $2\mu + E$ (Left panel) and $2\pi + E$ (right panel) in our model.

For $2M_\pi < M_s < 1$ GeV the Higgs boson can have spectacular decays from the chain $h \to ss \to \pi\pi(\mu\mu) + \pi\pi(\mu\mu)$ or $h \to ss \to \pi\pi(\mu\mu) + E$ and the missing energy E originates from one s decaying into $\omega\omega$ and hence is recoiling against the pair of detected particles. We did not include kaon modes since they are kinematically suppressed.

The $h \to 4\mu$ is particularly interesting and has been searched for by the CMS Collaboration [30]. The cross section is given by

$$\sigma(h \to 4\mu) = \sigma(h)\mathrm{Br}(h \to ss)[\mathrm{Br}(s \to \mu\mu)]^2. \quad (34)$$

For $2m_\mu < M_s < 2m_\pi$, $\mathrm{Br}(s \to \mu\mu) \lesssim 0.05$ and the CMS limit of $\sigma(h \to 4\mu) < 0.86$ fb at 95% C.L. implies $\Gamma(h \to ss) \lesssim 9.3 \times 10^{-2}$ MeV if the values $\sigma(h) = 15.13$ pb and $\Gamma_H = 4.07$ MeV are used. For $2m_\pi < M_s < 1$ GeV, $\mathrm{Br}(s \to \mu\mu) \approx 0.01$ and we have instead $\Gamma(h \to ss) \lesssim$ 2.3 MeV. Basically the current CMS limit post no constraint on this model. This is shown in Fig. 16. Interestingly the cross section for $2\mu + E$ is almost two orders of magnitude larger than that for 4μ by virtue of the larger invisible s branching ratio and this is given by

$$\sigma(h \to 2\mu + E) = 2\sigma(h)\mathrm{Br}(h \to ss)\mathrm{Br}(s \to \mu\mu) \times \mathrm{Br}(s \to \omega\omega). \quad (35)$$

The prediction of our model is displayed in Fig. 17. The largest branching ratios are around 10^{-6} and 10^{-5} for $2\mu + E$ and $2\pi + E$, respectively. For LHC14 the gluon fusion Higgs production cross section is ~50 pb and hence the high luminosity option will give the necessary rates. However, the background is expected to be large. Better signal selection triggers will greatly improve the odds. Detail studies are beyond the scope of this paper. All these modes can also be searched for at the ILC or an e^+e^- Higgs factory where the background is much smaller and the events are cleaner. However, the Higgs production cross section at the e^+e^- machine is roughly 2 orders of magnitude smaller than that at the LHC. To see these rare Higgs decays at an e^+e^- collider, one needs ~100 times larger luminosity than the currently envisioned for these machines.[1]

VIII. CONCLUSIONS

We have augmented the minimal Majoron model for dark radiation with a SM singlet scalar endowed with unit lepton number. The spontaneous breaking of the global $U(1)_L$ has three important consequences: (1) the Goldstone Majoron can serve as DR, (2) the type-I seesaw mechanism for light neutrino masses can be implemented, and (3) a Z_2 dark parity naturally occurs as a residual symmetry. The existence of a stable scalar dark matter is thus natural. Since the new physics introduced is in the form of SM singlet scalars, they interact with the SM fields with the Higgs boson as the mediator. In order to obtain an acceptable value for ΔN_{eff}, that characterizes DR, it is found that the Majoron must decouple at temperature around m_μ although the exact value is not predicted. This leads to the existence of a light scalar s that mixes with the SM Higgs boson. In turn it results in spectacular rare Higgs boson decays such as displaced vertices and muon pairs with missing energy recoiling against the pair themselves. These can be searched for at the LHC. The invisible width of the Higgs boson is also enhanced which perhaps is best measured at an e^+e^- Higgs factory. Our numerical analysis also reveals that the lepton number violating scale v_s is in the range of 1 TeV $< v_s <$ 100 TeV. This gives additional motivation to search for heavy neutrinos at the LHC. Again, a TeV e^+e^- colliders such as CLIC will be more suitable. Certainly we are encouraged that the seesaw scale is not hopelessly out of reach.

We have also investigated whether the model can accommodate the reported gamma-ray excess from the Galactic

[1]We thank Jessie Shelton for pointing out to us our earlier overly optimistic estimation.

center. This can come from $\rho\rho \to ss$ followed by s decaying into light hadrons. We found that a $\sim$40 GeVρ can be made consistent with the data. However, tension with rare B-meson decays is also present. This can be resolved by making the mixing of s and the Higgs boson very small and also increasing the decoupling temperature.

In conclusion we constructed a minimal model of Majoron dark radiation with a scalar dark matter that satisfies all experimental constraints. It also has interesting Higgs phenomenology that can be pursued at the high luminosity LHC and a future super e^+e^- Higgs factory.

ACKNOWLEDGMENTS

W. F. C. was supported by the Taiwan MOST under Grant No. 102-2112-M-007-014-MY3. J. N. N. is partially supported by the NSERC of Canada.

[1] G. Mangano, G. Miele, S. Pastor, T. Pinto, O. Pisanti, and P. D. Serpico, Nucl. Phys. **B729**, 221 (2005).
[2] P. A. R. Abe *et al.* (Planck Collaboration), arXiv:1303.5076.
[3] A. G. Riess, L. Macri, S. Casertano, H. Lampeitl, H. C. Ferguson, A. V. Filippenko, S. W. Jha, W. Li, and R. Chornock, Astrophys. J. **730**, 119 (2011); **732**, 129(E) (2011).
[4] G. Hinshaw *et al.*, Astrophys. J. Suppl. Ser. **208**, 19 (2013).
[5] J. L. Sievers *et al.*, J. Cosmol. Astropart. Phys. 10 (2013) 060.
[6] Z. Hou *et al.*, Astrophys. J. **782**, 74 (2014).
[7] S. Weinberg, Phys. Rev. Lett. **110**, 241301 (2013).
[8] W.-F. Chang, J. N. Ng, and J. M. S. Wu, Phys. Lett. B **730**, 347 (2014).
[9] Y. Chikashige, R. N. Mohapatra, and R. D. Peccei, Phys. Lett. B **98**, 265 (1981); J. Schechter and J. W. F. Valle, Phys. Rev. D **25**, 774 (1982).
[10] P. Minkowsky, Phys. Lett. B **67**, 421 (1977); T. Yanagida, in *Proceedings of Workshop on Unified Theories* (KEK, 1979), pp. 79 and 95; M. Gell-Mann, P. Ramond, and R. Slansky, in *Supergravity*, edited by P. van Niewenhuizen and D. Freedman (North Holland, Amsterdam, 1979), p. 315; S. L. Glashow, in *Cargese Summer Institute on Quarks and Leptons*, edited by M. Levy (Plenum Press, N.Y. 1980), p. 687; R. N. Mohapatra and G. Senjanovic, Phys. Rev. Lett. **44**, 912 (1980); J. Schechter and J. W. F. Valle, Phys. Rev. D **22**, 2227 (1980).
[11] A. Melchiorri, O. Mena, S. Palomares-Ruiz, S. Pastori, A. Slosar, and M. Sorel, J. Cosmol. Astropart. Phys. 01 (2009) 036.
[12] L. A. Anchordoqui, H. Goldberg, and G. Steigman, Phys. Lett. B **718**, 1162 (2013).
[13] K. Nakayama, F. Takahasi, and T. T. Yanagida, Phys. Lett. B **697**, 275 (2011).
[14] M. Blennow, E. F. Martinez, O. Mena, J. Redondo, and P. Serra, J. Cosmol. Astropart. Phys. 07 (2012) 022.
[15] J. Hasenkamp, arXiv:1405.6736.
[16] W.-F. Chang, J. N. Ng, and J. M. S. Wu, Phys. Rev. D **86**, 033003 (2012).
[17] P. P. Giardino, K. Kannike, I. Masina, M. Raidal, and A. Strumia, J. High Energy Phys. 05 (2014) 046.
[18] A. Djouadi, Phys. Rep. **457**, 1 (2008).
[19] A. Crivellin, M. Hoferichter, and M. Procura, Phys. Rev. D **89**, 054021 (2014).
[20] L. A. Anchordoqui, P. B. Denton, H. Goldberg, T. C. Paul, L. H. M. da Silva, B. J. Vlcek, and T. J. Weiler, Phys. Rev. D **89**, 083513 (2014).
[21] D. S. Akerib *et al.* (LUX Collaboration), Phys. Rev. Lett. **112**, 091303 (2014).
[22] T. Daylan, D. P. Finkbeiner, D. Hooper, T. Linden, S. K. N. Portillo, N. L. Rodd, and T. R. Slatyer, arXiv:1402.6703.
[23] A. Martin, J. Shelton, and J. Unwin, arXiv:1405.0272.
[24] L. Bergstrom, P. Ullio, and J. H. Buckley, Astropart. Phys. **9**, 137 (1998); J. L. Feng, K. T. Matchev, and F. Wilczek, Phys. Rev. D **63**, 045024 (2001).
[25] B. Pratt and F. Wilczek, arXiv:hep-ph/0605188.
[26] W. F. Chang, J. N. Ng, and J. M. S. Wu, Phys. Rev. D **75**, 115016 (2007).
[27] M. J. Strassler and K. M. Zurek, Phys. Lett. B **661**, 263 (2008).
[28] A. Kumar, J. N. Ng, A. Spray, and P. T. Winslow, Phys. Rev. D **88**, 075012 (2013).
[29] J. C. Helo and S. G. Kovalenko, Phys. Rev. D **89**, 073005 (2014).
[30] CMS Collaboration, Phys. Lett. B **726**, 564 (2013).